FISEVIER

Contents lists available at ScienceDirect

Flow Measurement and Instrumentation

journal homepage: www.elsevier.com/locate/flowmeasinst



A Pitot tube system for obtaining water velocity profiles with millimeter resolution in devices with limited optical access



Ronald J. Lynn ^a, Igor V. Haljasmaa ^a, Frank Shaffer ^b, Robert P. Warzinski ^b, Jonathan S. Levine ^{b,*}

- a URS, South Park, PA 15129, USA
- ^b U.S. Department of Energy, National Energy Technology Laboratory, P.O. Box 10940, Pittsburgh, PA 15236, USA

ARTICLE INFO

Article history:
Received 19 February 2014
Received in revised form
13 August 2014
Accepted 19 August 2014
Available online 27 August 2014

Keywords:
Miniature S-type Pitot tube
Water velocity profiles
Automation
High-pressure water tunnel
Fine spatial resolution
Low-pressure calibration system

ABSTRACT

An automated, miniature, S-type Pitot tube system was created to obtain fluid velocity profiles at low flows in equipment having limited optical access, which prevents the use of standard imaging techniques. Calibration of this non-standard Pitot tube at small differential pressures with a custom, low-pressure system is also described. Application of this system to a vertical, high-pressure, water tunnel facility (HWTF) is presented. The HWTF uses static flow conditioning elements to stabilize individual gaseous, liquid, or solid particles with water for optical viewing. Stabilization of these particles in the viewing section of the HWTF requires a specific flow field, created by a combination of a radially expanding test section and a special flow conditioner located upstream of the test section. Analysis of the conditioned flow field in the viewing section of the HWTF required measurements across its diameter at three locations at 1 mm spatial resolution. The custom S-type Pitot tube system resolved pressure differences of < 100 Pa created by water flowing at 5–30 cm/s while providing a relatively low response time of \sim 300 s despite the small diameter (< 1 mm) and long length (340 mm) of the Pitot tube needed to fit the HWTF geometry. Particle imaging velocimetry measurements in the central, viewable part of the HWTF confirmed the Pitot tube measurements in this region.

© 2014 Elsevier Ltd. All rights reserved.

1. Introduction

1.1. Experimental system and motivation

The HWTF at the National Energy Technology Laboratory was designed to study the chemistry, physics, and hydrodynamics of rising or sinking fluid particles at deep ocean conditions, simulating water depths to 3400 m and temperatures down to freezing [1–3]. A vertical, countercurrent water flow is used to stabilize gaseous, liquid, or solid particles in a viewing window for minutes to hours while video-based measurements are made. Vertical positioning of a particle in a window of a viewing section (VS in Fig. 1) is achieved by countering its natural buoyancy with a controlled water flow through a tapered, conical, plastic insert in the VS that causes the water velocity to decrease with increasing diameter. A custom flow conditioner (Fig. 1 inset) located upstream of the test section creates a velocity minimum near the vertical axis of the VS that provides radial stabilization of a particle in the VS. Particles up to about 20 mm diameter have sufficient freedom to permit a measure of natural hydrodynamics to be observed, in particular, wake-induced lateral path and shape oscillations. Experimental times can be long enough for kinetic experiments and dissolution measurements.

The HWTF was originally used to determine the dissolution rates of both rising and sinking liquid carbon dioxide drops, with and without clathrate hydrate shells, and sinking carbon dioxide/hydrate/seawater particles [2,3]. The system is currently being used for experiments on less-dense hydrocarbon gases. At deep ocean conditions, the densities of light hydrocarbon gas bubbles ($\sim 50-350 \text{ kg/m}^3$) are lower than liquid CO₂ drops ($\sim 700-1050 \text{ kg/m}^3$) and therefore travel faster through an aqueous phase ($\sim 1000-1030 \text{ kg/m}^3$), which results in increased oscillatory behavior. Correlation of bubble hydrodynamics with rise velocity requires detailed radial profiles of the mean water velocity in the vicinity of the viewing window in the VS of the HWTF. This information is also necessary to design the upstream flow conditioner and assess how particular profiles affect bubble stability.

1.2. System constraints and requirements

The high-pressure design requirements of the HWTF limits the use of standard off-the-shelf equipment for determining velocity profiles in the VS. Hot wire/hot film anemometers were rejected because of

^{*} Corresponding author. Tel.: +1 412 386 7534. E-mail address: Jonathan.Levine@netl.doe.gov (J.S. Levine).

Nomenclature	V volume (m ³) V_d volume change at the DPT diaphragm (m ³)
surface area (m ²) gravitational acceleration (m s ⁻²) height (m) e exponential time constant for the DPT (s ⁻¹) exponential time constant following Preston's hydrostatic design (s ⁻¹) length (m)	Greek symbols $\mu \qquad \text{dynamic viscosity (Pa s)} \\ \rho \qquad \text{density (kg m}^{-3}\text{)}$ Subscripts
P pressure (Pa) ΔP differential pressure (Pa) Q(t) volumetric flow rate (m ³ s ⁻¹) P radius (m) P Reynolds number P t time (s) P velocity (m s ⁻¹)	 f full scale m measured 0 equilibrium value w water

concerns regarding contamination, ambient system temperature fluctuations, and relative fragility due to the higher density and viscosity of water compared to more typical applications in gas systems. Laser Doppler anemometry and particle imaging velocimetry (PIV) techniques are limited by the size of optical access windows that would permit visual observation of only a portion of the HWTF VS. A Pitot tube represented the best option in terms of simplicity, reliability, and cost; however, a custom design and associated calibration would be required to accommodate the HWTF geometry and application requirements. The 96.5-mm-thick walls of the HWTF do not permit the use of an L-type Pitot tube, therefore, an S-type was chosen.

Typical water velocities determined by Pitot tubes are on the order of meters per second [4,5]. However, the vertical water velocities used in the HWTF to stabilize a hydrocarbon bubble are on the order of 10–30 cm/s, resulting in a small differential pressure signal. For a velocity range of 0–30 cm/s, assuming an S-type Pitot tube factor of 0.8, the full-scale differential pressure, ΔP , is only

$$\Delta P = \frac{1}{(0.8)^2} \frac{\rho_w v^2}{2} = \frac{(1000 \frac{\text{kg}}{\text{m}^3})(0.3 \frac{\text{m}}{\text{s}})^2}{1.28} = 70 \text{ Pa} = 7.1 \text{ mmH}_2\text{O}$$
 (1)

where ρ_w and v are water density and velocity, respectively. This requires a sensitive differential pressure device with an accuracy of 1 Pa (\sim 0.1 mmH₂O) or better.

A long, narrow Pitot tube is required to access the interior of the HWTF VS. Narrow Pitot tubes are not typically used for measurements in water owing to long equilibration times. For example, Preston [6] describes a Pitot tube system for velocity determinations down to 3 cm/s in a water system. To mitigate surface tension and temperature-change effects, this system required large water reservoirs that resulted in response times of more than an hour per data point for 1 mm ID Pitot tubes (see Appendix A), making this method impractical in the HWTF. To reduce signal equilibration time, a Pitot tube system would need to eliminate air—water interfaces and have minimal water displacement volume.

Another limitation of using Pitot tubes for determination of slow flows is an error in velocities at low Reynolds numbers (Re) due to viscous effects. Boetcher and Sparrow [7] showed that viscous effects become non-negligible for Re < 100 (based on the Pitot tube outer diameter), and cause a 2–5% velocity error for Re < 50.

Based on the above, an S-type Pitot tube capable of low-velocity determinations in water in the HWTF VS requires

- differential pressure measurement accuracy of \sim 1 Pa or better,
- avoidance of air-water interfaces,
- a measuring device with a minimal volumetric displacement and
- sufficient velocities to avoid viscous effects.

2. Materials and methods

2.1. Pitot tube system design and incorporation into the HWTF

The HWTF has 96.5-mm-thick walls in the viewing region and small diameter access ports that preclude the use of an L-type tube. Four high-pressure windows are located 90° apart around the midpoint of each windowed VS (Fig. 1). They consist of two opposed 40 mm, circular windows and two opposed 12.7-mm-wide by 152.4-mm-long, oblong windows. A metal insert with five 6.4 mm diameter ports was made to replace one of the oblong windows and provide access for a Pitot tube (see inset b in Fig. 2), which moves through the insert via an O-ring seal in a bored-through, 6.4-mm-female by 1/4″-NPT-male Swagelok fitting. Similar fittings were used to cap unused ports in the metal insert.

Velocity determinations were needed at different heights in the VS to understand how the velocity profile created by the flow conditioner develops through the HWTF test section. Measurements were performed through the top, middle, and bottom 6.4 mm diameter ports located in the metal insert (Fig. 2). The middle port was located at the same height as the center of the circular viewing window, 190.5 mm downstream of the VS inlet. The top and bottom ports were located 57.15 mm above and below the middle port, respectively, as measured from the center of each port. In Figs. 1 and 2, the Pitot tube is shown mounted in the middle port. The tapered, plastic, flow-conditioning insert indicated in Fig. 2 has cutouts that match the window openings in the VS and measurements extended into this region.

With the present optics, the smallest diameter object that can be positioned in the VS for observation is about 1 mm, setting both the required velocity profile resolution and the maximum inner diameter (ID) of the Pitot tube capillaries. Smaller capillary IDs also reduce errors caused by velocity gradients, called the "apparent shift in Pitot location" (see [8] and references therein). However, IDs much smaller than 1 mm dramatically increase response times (Appendix A) and may lead to clogging. The Pitot tube also had to be long enough to penetrate the HWTF walls and traverse the entire test section, causing longer response times (Appendix A).

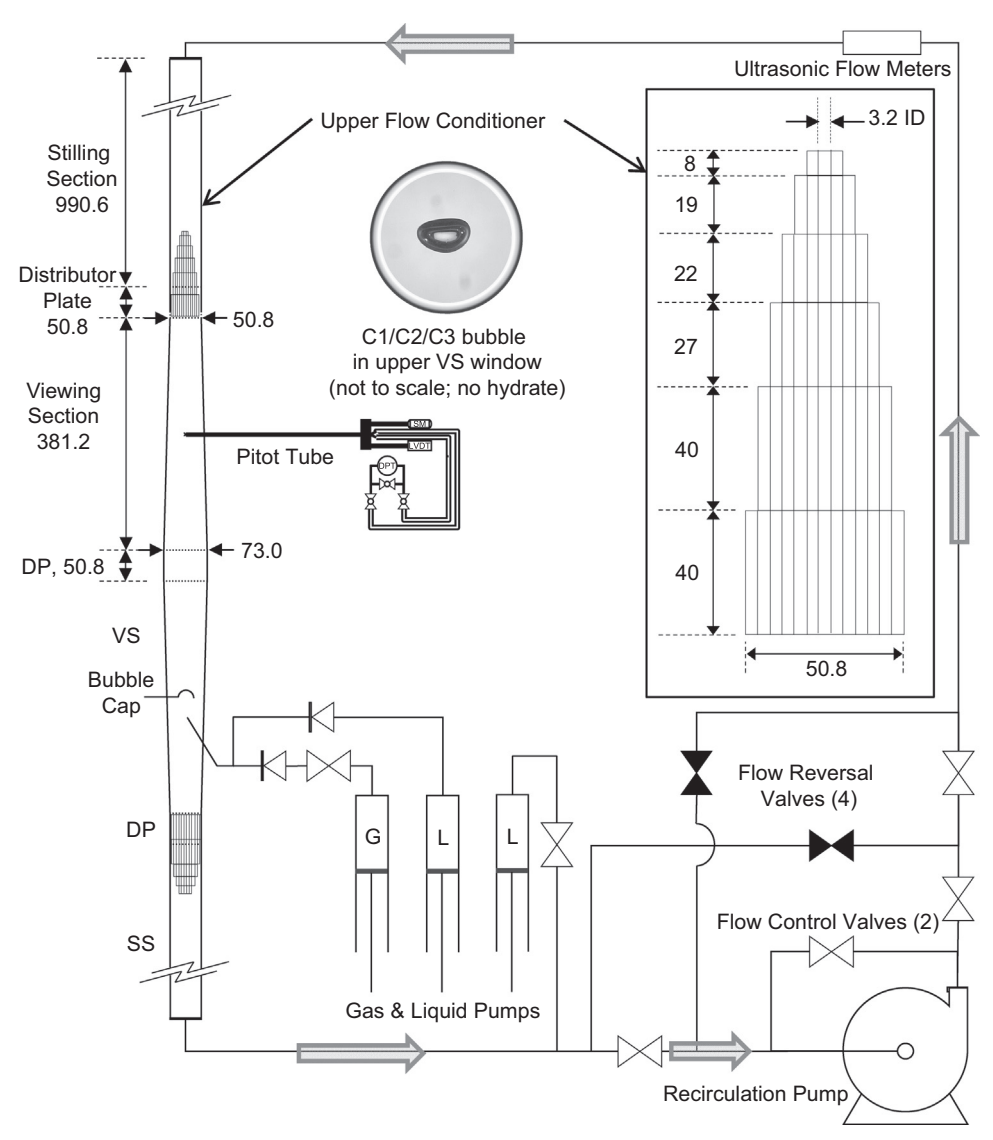


Fig. 1. Schematic of the high-pressure water tunnel facility (HWTF) showing the Pitot tube system (details in Figs. 2 and 3). Dimensions in mm. The water tunnel (WT), on the left in the diagram, consists of two windowed viewing sections (VS), two stilling sections (SS), and three distributor plates (DP) that join these sections and provide various access ports (see Ref. [3] for details). The diagram only shows the interior geometry of the WT, the pressure shell is omitted. Window details are in Section 2.1. The top center inset shows a methane, ethane, propane (C1C2C3) bubble stabilized in the HWTF by a downward flow of water.

With these constraints, an S-type Pitot tube was made that consisted of a pair of 0.76 mm ID, 1.6 mm OD, 340-mm-long, stainless steel, capillary tubes that were epoxy-sealed in a 6.4 mm OD tube. The S tip of the Pitot tube was handmade and is shown in inset a of Fig. 2. The capillary tube ends were fitted with Swagelok fittings that permitted connection to Clearflex V60 PVC tubing (15.9 mm OD, 6.4 mm ID). The S-type Pitot tube was previously calibrated against a standard 3.175 mm, L-type Pitot tube (Dwyer Instruments) in a low-pressure water tunnel constructed of plastic with similar internal dimensions and flow capacities as the HWTF [9].

As discussed in Section 1, significant viscous effects are avoided if Re > 50. The Re for water with the characteristic length, L, set by the 1.6 mm OD capillary tubing used to make the Pitot tube, is

$$Re = \frac{\rho_w vL}{\mu_w} = \frac{(10^3 \text{ kg/m}^3)(0.00 \text{ 16 m})v}{(10^{-3} \text{ Pa s})} = 1600v$$
 (2)

where μ_w is the dynamic viscosity of water. Hence, to avoid viscous effects, the lowest velocity, ν , should be about 3 cm/s. 5 cm/s was chosen for the lower limit on velocity to provide a

safety margin given the unknown differences between S-type and L-type Pitot tubes. Water velocities in the HWTF are above the viscous range, typically 10–30 cm/s.

2.2. Differential pressure transducer and its calibration

The pressure drop across the Pitot tube was measured with a Validyne DP103-08 differential pressure transducer (DPT) (55 Pa full range, 0.25% accuracy) that provides the required sensitivity, measures a wet–wet differential pressure, thus avoiding an air–water interface, and has a volumetric displacement of 57 μL . The DPT was connected to a Validyne CD23A-1E1C signal conditioner. The voltage was manually zeroed before each calibration or set of velocity profile determinations in the HWTF by connecting the two sides of the DPT via 4.6 mm OD, stainless steel tubing (Fig. 3) to ensure hydrostatic equilibrium. A baseline voltage correction was also made at each horizontal location using measurements taken at zero flow at the beginning and end of measurements at each system height.

The DPT was calibrated using the setup shown in Fig. 3. Each side of the transducer was connected via 6.4 mm OD, 4.6 mm ID,

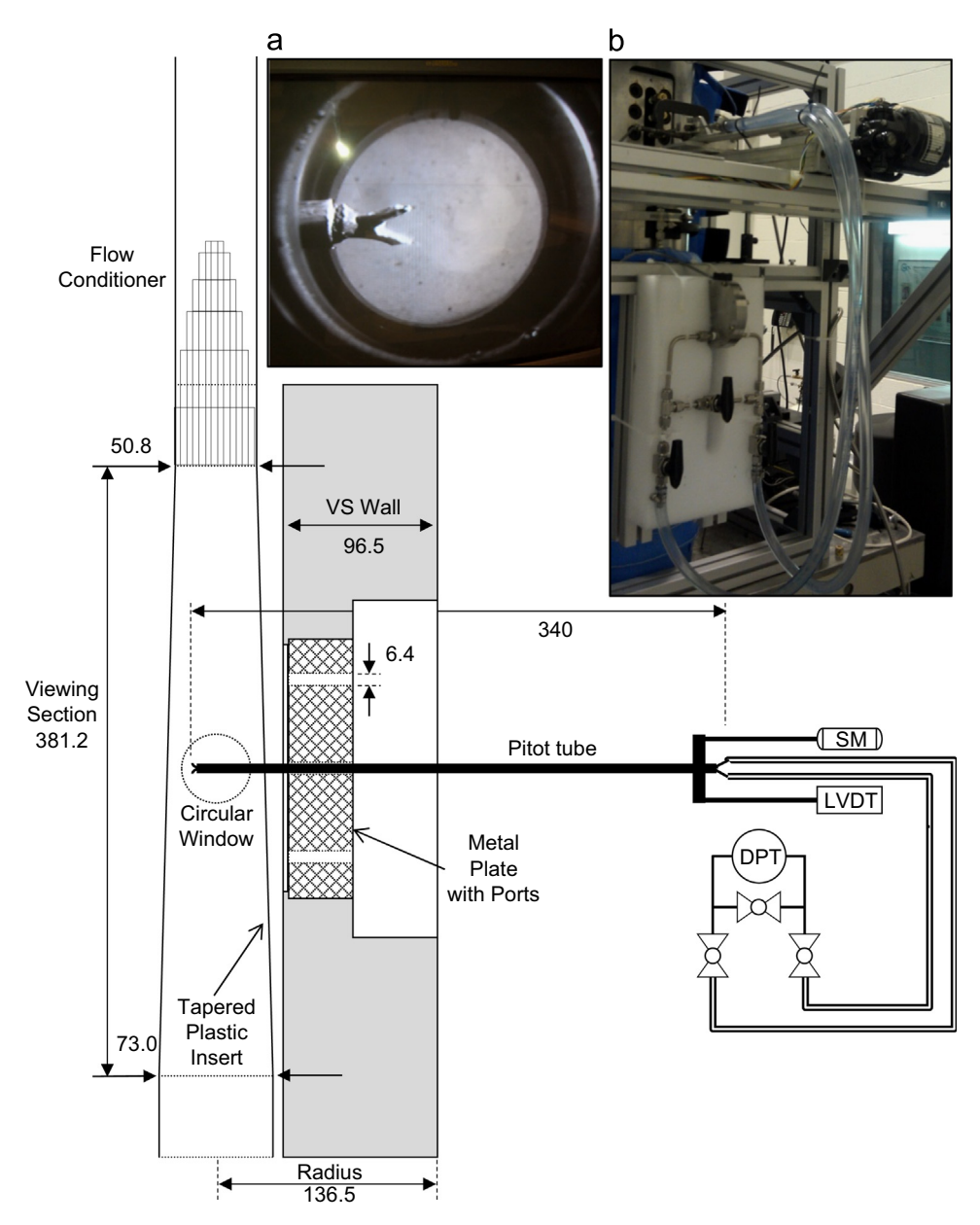


Fig. 2. Schematic and photographs depicting the Pitot tube system and its connection to the HWTF. The drawing shows the Pitot tube entering the VS through the middle port in the metal insert. See Section 2.1 for details. Mounting hardware is not shown. All dimensions are in mm. The connection of the Pitot tube to the DP transducer is also shown (not to scale). Fig. 3 contains detail on the DP transducer assembly. The photograph in inset a shows the end of the handmade, S-type Pitot tube. Inset b contains a picture of the Pitot tube system connected to the middle port of the metal insert in one of the oblong windows of the HWTF with the DP transducer assembly below it.

stainless steel tubing to the Clearflex $^{\text{TM}}$ V60 PVC tubing to large 24 mm ID, transparent, water reservoirs, each mounted on an Edmund Optics EDM-37979 micrometer linear translation stage (0.0020 mm linear accuracy, 0.0013 mm repeatability). Before calibration, a valve (Swagelok SS-43S4) is opened to ensure hydrostatic equilibrium across the DPT. By varying the height of one of the water reservoirs, a series of known hydrostatic pressures can be produced within the full range of the transducer. The resulting accuracy is 2 μ m on a full-scale range of 5.6 mmH₂O (0.035%).

During calibration measurements, displacement of water by the diaphragm can cause an error in the data by raising the water level in one of the reservoirs and lowering it in the other. The manufacturer specifies a 57 μ L displacement volume at full scale, corresponding to a 0.126 mm change in water level in the 24 mm ID water reservoirs used for calibration. This would represent a 4.5% error in the calibration data (details in Appendix B).

The calibration data were therefore corrected for the diaphragm displacement, assuming the same percentage error through the range of the DPT. Fig. 4 shows the voltage vs. hydrostatic pressure calibration data with and without this correction.

This calibration method is straightforward and uses readily available equipment. This DPT incorporates a thin diaphragm that is easily damaged; hence it was necessary to be able to easily and quickly recalibrate the transducer on site. Offsite calibration is also questionable owing to the delicate nature of the diaphragm. The calibration method presented here avoids these concerns. Its accuracy relies only on the precision of the linear translation stages.

2.3. Automated system and software control

A single velocity profile at 1 mm spatial resolution across the $\sim\!80$ mm diameter of the HWTF tapered test section, with both

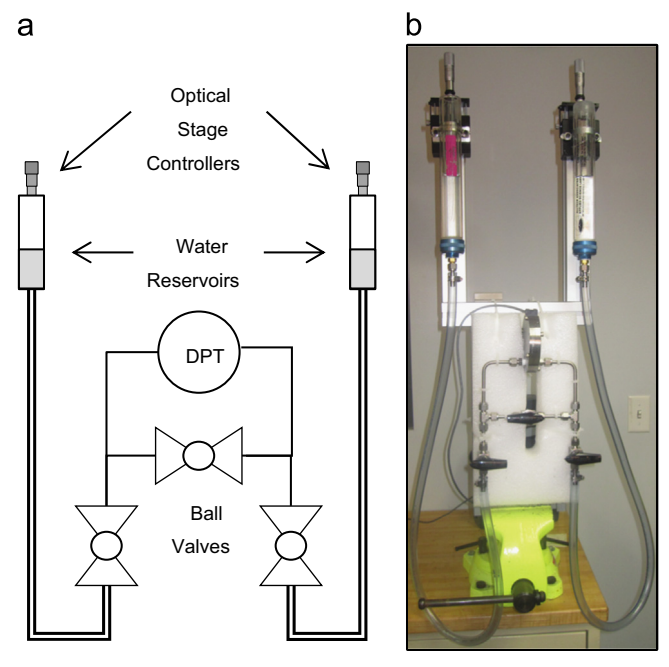


Fig. 3. Schematic (a) and photograph (b) of the DPT calibration system. The displacement volume of the DPT's diaphragm was determined by replacing one of the water reservoirs with a 5.5 mm ID capillary tube.

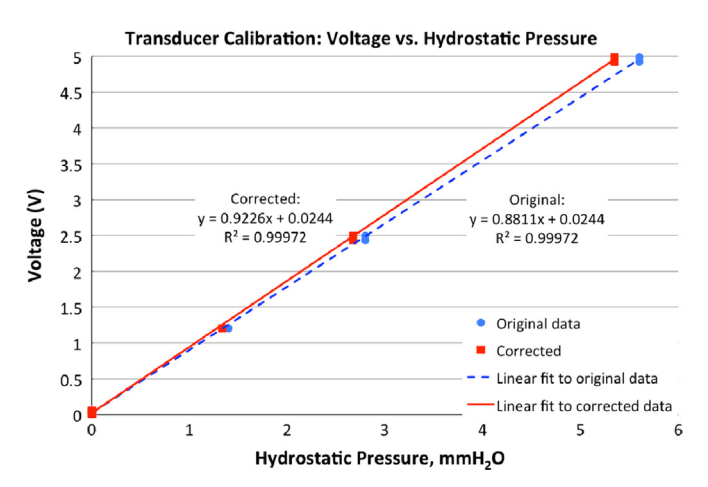
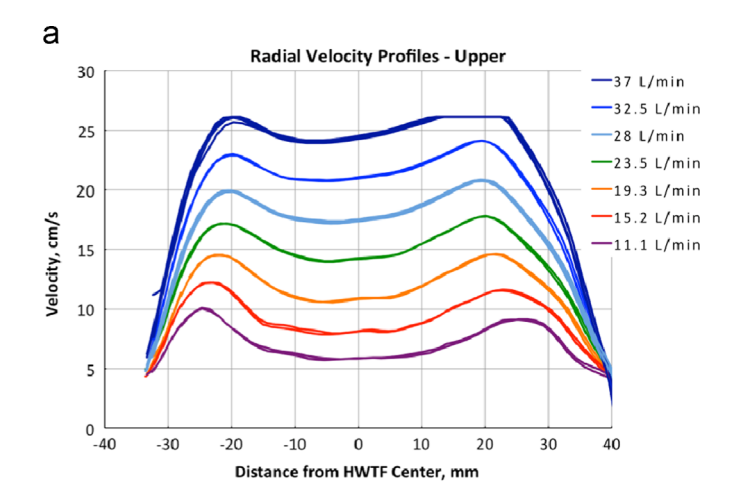


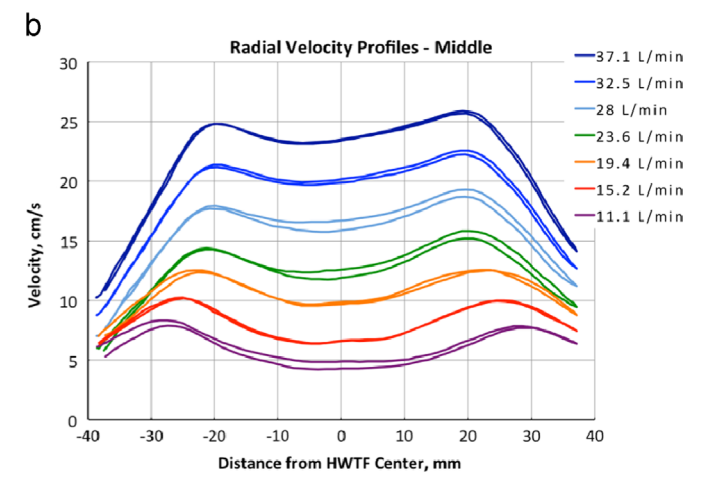
Fig. 4. Voltage vs. hydrostatic pressure calibration data with and without the diaphragm volumetric displacement correction.

forward and reverse traversing measurements for confirmation, consisted of 158 data points. Velocity profiles were obtained at three heights in the test section at seven flow rates for a total of 3318 measurements. A LabVIEW virtual instrument (VI) was developed to automate the measurement process.

The horizontal position of the Pitot tube inside the HWTF is controlled by an automated translation system. The distance between experimental points is measured by a linear variable differential transformer (LVDT) (Transtek, 0.1% accuracy) connected to a potentiometer signal conditioning system (Transtek 1000–0012). A computer-controlled stepper motor uses feedback from the LVDT to move the Pitot tube in 1 mm increments at regular time intervals set by the system equilibration time, which is about 5 min (Appendix A). The signal acquisition time is 1 s, which is negligible by comparison, with an average sampling rate of 100 Hz.

Velocity profiles were determined at flow rates from 11 to 37 L/\min that were set by changing the HWTF recirculation pump





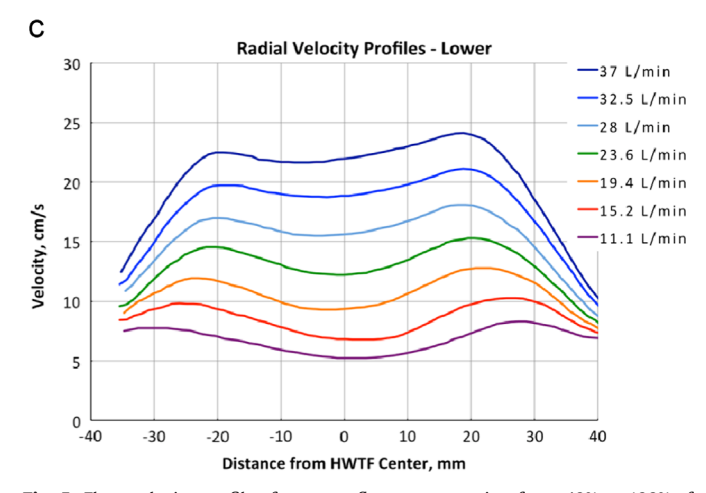


Fig. 5. Flow velocity profiles for pump flow rates ranging from 40% to 100% of pump capacity in 10% increments with the Pitot tube in the (a) top, (b) mid-section, and (c) bottom ports of the metal insert. The reverse profiles were not obtained at the bottom port (c).

(Fig. 1) speed from 40% to 100% at 10% intervals. The lowest speed was above the 5 cm/s limit, below which viscous effects can occur. The volumetric flow rate was determined independently elsewhere in the system with a pair of ultrasonic flow meters with an accuracy of 1% of flow (Fig. 1) [3]. Each of the 3 sets of velocity profiles required several days to perform. The LabVIEW VI automatically controlled the pump speed, incremented horizontal position in the tunnel, paused for the predetermined equilibration

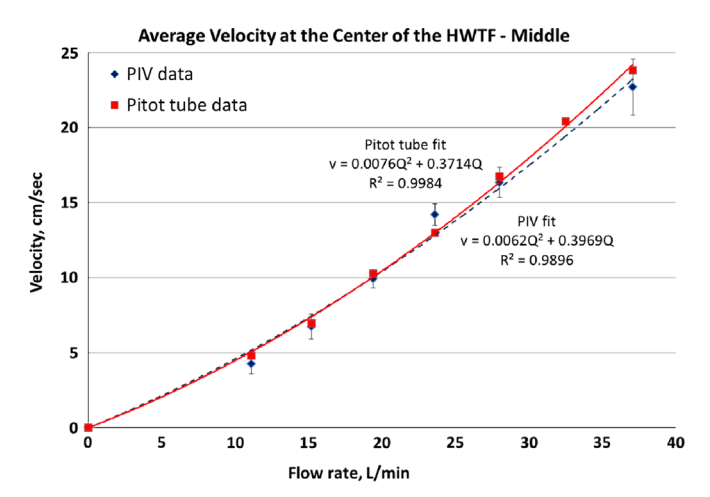


Fig. 6. Verification of Pitot tube velocity determinations by comparison with PIV measurements at the circular optical window in the VS. Pump flow rates from $11\ L/min$ to $37\ L/min$ are compared. Pitot tube data are from Distance point 0 in Fig. 5b. A quadratic equation represents the fit of flow rate vs. velocity based on the Pitot tube data. Error bars of one standard deviation are shown for the PIV data.

time, recorded location and differential pressure, and then moved to the next horizontal position.

3. Results and verification

The results for the S-type Pitot tube velocity profile determinations at seven pump speeds are shown in Fig. 5 for three different heights in the VS. Each velocity profile across the HWTF consisted of measurements made at 79 horizontal positions with 1 mm spacing. The measurements were performed in both the forward and reverse directions for the top and middle positions shown in Fig. 5a and b, respectively. The velocity profiles at the bottom position (Fig. 5c) were only performed in the forward direction. The highest velocities (Fig. 5, upper profile, 37 L/min) produced differential pressures above the range of the differential pressure cell, but within its overpressure limit of 110 Pa.

All three sets of velocity profiles show the desired broad and mild velocity minimum in the central part of the profile. The contribution to vertical stabilization caused by the taper of the test section can also be seen by comparing the velocity profiles at different heights, with slower velocities as cross-sectional area increases downstream.

A particle imaging velocimetry (PIV) system developed at NETL [10,11] was used in a separate experiment to independently validate the Pitot tube data (Fig. 6). The PIV measurements tracked ≤ 100 µm, liquid propane drops and mixed methane/propane hydrate particles formed in the HWTF at 1.9 °C and 15.1 MPa that served as near-neutrally-buoyant tracers in the water flow. The PIV data were limited to the viewable volume located in the central part of the middle transect that can be seen from the circular window in the VS. A Vision Research v341 high-speed camera was used to record images of these tracers in a plane through a circular window in the center of the VS. The thickness of the plane was approximately 1 cm and was set by using a wide aperture lens. ImageJ [12] was used for image enhancement and location of tracer centroids. The PIV measurement accuracy is ± 1 pixel for particles traversing on the order of 500 pixels, providing a 0.2% linear accuracy. The good agreement (\pm 5%) between the Pitot tube and PIV data in this region is evident in Fig. 6. The two velocity determination systems are also highly complementary in this application, with the Pitot tube providing flow profiles at 3 heights spanning 11.43 cm of the central region in the upper VS of the HWTF (Fig. 2) and PIV providing data at finer horizontal and temporal scales in the central viewing region where bubble stabilization is desired.

4. Conclusion

A novel, miniaturized, S-type Pitot tube system and specialized calibration equipment and protocols were developed that enabled determination of relatively low (5-30 cm/s) water velocities that are necessary for stabilizing buoyant gas and liquid particles in a high-pressure, counter-flowing system. The Pitot tube and calibration system development were presented in the context of a project involving NETL's HWTF in which buoyant hydrocarbon particles are studied at deepwater conditions. From previous work, the desired flow profile for stabilizing a particle required a velocity profile with a slower flow in the central region of the HWTF. The results reported here demonstrated successful use of the S-type Pitot tube and calibration system and confirmed that the HWTF flow-conditioning elements successfully created such a profile. The Pitot tube data were also independently validated using optical particle tracking methods in the central region of the HWTF.

The custom Pitot tube and calibration system overcame design challenges related both to the low-velocity water flows and the geometrical constraints of the HWTF unit. These challenges include a 1 mm spatial resolution, < 100 Pa differential pressures, and avoidance of air–water interfaces to minimize volumetric displacement in the measurement device. The system was also automated to facilitate positioning of the Pitot tube and data collection. Utilizing the information presented here, implementation of similar strategies would enable determination of velocity profiles in other devices with limited optical access.

Disclaimer

This report was prepared as an account of work sponsored by an agency of the United States Government. Neither the United States Government nor any agency thereof, nor any of their employees, makes any warranty, express or implied, or assumes any legal liability or responsibility for the accuracy, completeness, or usefulness of any information, apparatus, product, or process disclosed, or represents that its use would not infringe privately owned rights. Reference herein to any specific commercial product, process, or service by trade name, trademark, manufacturer, or otherwise does not necessarily constitute or imply its endorsement, recommendation, or favoring by the United States Government or any agency thereof. The views and opinions of authors expressed herein do not necessarily state or reflect those of the United States Government or any agency thereof.

Acknowledgments

This work was supported by the Department of Energy Complementary Research Program under Section 999 of the Energy policy Act of 2005 and by the Department of Interior, Bureau of Safety and Environmental Enforcement under Interagency Agreement M11PG00053. Support for Jonathan Levine came through the Oak Ridge Institute for Science and Education Postgraduate Research Program at NETL.

Appendix A. System equilibration times

Calculations of system equilibration times were necessary to determine if the measurement system presented in Preston [6] was viable for use with the HWTF's constrained geometries, as well as to assess the resulting improvement.

Based on Preston's design with our S-type Pitot tube, equilibration time is limited by the time required for water to move through the 0.76 mm ID, Pitot tube capillaries that were used and into or out of water reservoirs that would be connected to the DP transducer. In [6] these water reservoirs had large surface areas to mitigate errors due to air–water interfaces, requiring a relatively large volumetric flow through both Pitot tube capillaries for the system to re-equilibrate during each consecutive measurement. The pressure differential driving this flow, $\Delta P(t)$, decays with time, t, resulting in a change of reservoir height, h, due to Hagen–Poiseuille flow through the Pitot tube

$$\Delta P(t) = \rho_w gh(t) = \frac{8\mu L}{\pi r^4} Q(t) = \frac{8\mu LA}{\pi r^4} \frac{dh}{dt}$$
(A1)

where g is gravitational acceleration, Q(t) is volumetric flow rate, A is reservoir surface area, r is the inner radius of the Pitot tube capillaries and L is the sum of the length of both capillaries. Solving the differential equation, the combined level change in both reservoirs decays exponentially to a new equilibrium height, h_0 , as

$$h = h_0 \left[1 - \exp\left(-\frac{\pi r^4 \rho_w g}{8\mu L} t \right) \right] = h_0 [1 - \exp(-k_h t)]$$
 (A2)

where k_h is the exponential time constant for our system following Preston's hydrostatic design. Assuming reservoir areas, A, on the order of 10 cm^2 , and using the dimensions of our Pitot tube, r=0.375 mm, L=68 cm, the time constant would be

$$k_h = \frac{\pi r^4 \rho_w g}{8\mu L} = \frac{\pi (3.8 \times 10^{-4} \text{ m})^4 (10^3 \text{ kg/m}^3) (9.8 \text{ m/s}^2)}{8(10^{-3} \text{ Pa s})(0.68 \text{ m})(10^{-3} \text{ m}^2)} \approx 1.2 \times 10^{-4} \text{ s}^{-1}$$

Finally, assuming equilibrium when h reaches 98% of the new equilibrium value, h_0 , we can write

$$\frac{h_0 - h}{h_0} = 0.02 = \exp\left(-\frac{\pi r^4}{8\mu L}\frac{\rho_{\rm w}g}{A}t\right) = \exp(-k_h t) \tag{A4}$$

which gives an equilibration time of almost 9 h. This is an impracticably long signal acquisition time, corresponding to about 3.4 years for the 3318 measurements necessary.

The new design uses a DP transducer (Validyne DP103-08) with a low diaphragm displacement volume and no air–water interface, to minimize the equilibration time and therefore the total data collection time. We assume an exponential decay of the pressure differential to a new equilibrium value, ΔP_0 , as

$$\Delta P = \Delta P_0 \exp(-k_e t) \tag{A5}$$

where k_e is the exponential time constant for the electronic DP transducer design. Volume change at the diaphragm, V_d , must equal the integration of the flow rate over time, giving

$$V_d = \int_0^\infty Q(t)dt = \frac{\pi r^4 \Delta P_0}{8\mu L} \int_0^\infty \exp(-k_e t)dt = \frac{\pi r^4 \Delta P_0}{8\mu L} \frac{1}{k_e}$$
(A6)

Based on the transducer's rated accuracy of 0.25% in linearity and hysteresis we make the assumption that the volumetric deflection of the diaphragm is linearly proportional to the pressure difference, i.e. the ratio $\Delta P_0/V_d$ is constant (further details in Appendix B). The manufacturer specifies a volumetric displacement of 57 μ L at the full-scale pressure, i.e. V_d =57 μ L at

 $\Delta P_0 = 54.9 \text{ Pa } (5.6 \text{ mmH}_2\text{O}).$ The time constant is therefore

$$k_e = \frac{\pi r^4}{8\mu L} \frac{\Delta P_0}{\dot{V}_d} = \frac{\pi (3.8 \times 10^{-4} \text{ m})^4}{8(10^{-3} \text{ Pa s})(0.68 \text{ m})} \frac{54.9 \text{ Pa}}{5.7 \times 10^{-8} \text{ m}^3} \approx 0.012 \text{ s}^{-1}$$
(A7)

and the time for 98% decay to the new value is about 5.5 min. The equilibration time was verified experimentally and determined to be slightly less than 5 min, providing a total data acquisition time of just over 2 weeks. The new system is about two orders of magnitude faster owing to electronics and precision manufacturing techniques that have become available in the decades since [6]. Increasing the 0.76 mm Pitot tube inner diameters would reduce the equilibration time further due to the r^4 dependence, resulting in an equilibration time of \sim 1.8 min for 1 mm IDs and \sim 7 s for 2 mm IDs.

Appendix B. Correction for diaphragm displacement during transducer calibration

The calibration of the DP transducer requires a small correction for the volumetric displacement of the diaphragm. Although the displacement volume of the Validyne DP103-08 diaphragm is relatively small, reported as 57 μ L by the manufacturer, it corresponds to a height offset of 0.126 mm in the 24 mm ID water reservoirs used for the calibration (Fig. 3), \sim 2.25% of the full-scale hydrostatic pressure, 5.6 mmH₂O. This affects both reservoirs, and would therefore create an offset error of 4.5% at full-scale.

An identical displacement is listed for all the diaphragms available for this transducer despite the diaphragms having very different pressure sensing ranges, from 0.22 to 880 mmH₂O. To verify that the listed full-scale displacement volume was correct, we replaced one of the reservoirs with a 5.5 mm ID capillary tube to be able to precisely determine displacement volume. After establishing hydrostatic equilibrium, the large reservoir was set to a height 5.6 mm above the capillary tube reservoir by adjusting the micron stage and the volume of water displaced from the diaphragm was determined to be 35.6 µL. However, the displaced water raised the height of the water in the capillary by 1.5 mm, and therefore the true hydrostatic pressure on the diaphragm was 5.6-1.5 mm=4.1 mmH₂O. To scale the measured volumetric displacement to full-scale displacement we make the assumption that diaphragm volumetric displacement, V, is linearly proportional to the pressure, P

$$\frac{V_m}{V_f} = \frac{P_m}{P_f} \tag{B1}$$

where subscript m denotes measured and f denotes full scale. Under this assumption, the equivalent full-scale displacement volume is therefore

$$V_f = V_m \frac{P_f}{P_m} = 35.6 \mu L \left(\frac{5.6 \text{ mmH}_2 \text{O}}{4.1 \text{ mmH}_2 \text{O}} \right) = 48.6 \mu L$$
 (B2)

which is 85% of the manufacturer's specified displacement volume. The manufacturer specifies a 0.25% error due to non-linearity or hysteresis for this transducer giving some justification to this assumption. While linearity of the pressure–voltage relationship does not necessarily require linearity of displacement relative to pressure, any non-linearity would be expected to change the result less than a few percent. As the dimensions of the capillary ID, capillary rise height, and pressure–displacement relationship each have some associated error and the volume determined was within reasonable agreement of the manufacturer's specification, we use the manufacturer's specification for the full-scale diaphragm volumetric displacement: 57 µL.

Under the assumption that the volumetric displacement of the diaphragm is linearly proportional to the differential pressure, the 4.5% correction for error caused by the displacement volume is applied to the entire calibration, as shown in Fig. 4. The error associated with a non-linearity of a few percent of this 4.5% correction would be < 0.1%, less than errors associated with, e.g., the accuracy of the signal acquisition equipment, and thus would not affect the result.

A correction for the diaphragm displacement volume could be avoided by using larger-area water reservoirs during calibration, at the cost of increasing calibration signal acquisition time. Tripling the reservoir IDs would have reduced the correction to $\sim\!0.5\%$ while increasing the calibration time negligibly compared to the setup time.

References

- [1] Haljasmaa IV, Vipperman JS, Lynn RJ, Warzinski RP. Control of a fluid particle under simulated deep-ocean conditions in a high-pressure water tunnel. Rev Sci Instrum 2005;76:025111. http://dx.doi.org/10.1063/1.1854216.
- [2] Warzinski RP, Lynn RJ, Haljasmaa I, Zhang Y, Holder GD. Dissolution of CO₂ drops and CO₂ hydrate stability under simulated deep ocean conditions in a

- high-pressure water tunnel. In: Proceedings of the third annual conference on carbon capture and sequestration. Alexandria, Virginia; 2004.
- [3] Warzinski RP, Riestenberg DE, Gabitto J, Haljasmaa IV, Lynn RJ, Tsouris C. Formation and behavior of composite CO₂ hydrate particles in a high-pressure water tunnel facility. Chem Eng Sci 2008;63:3235–48.
- [4] Mishra R, Singh S, Seshadri V. Velocity measurement in solid-liquid flows using an impact probe. Flow Meas Instrum 1998;8:157–65.
- [5] Magirl CS, Gartner JW, Smart GM, Webb RH. Water velocity and the nature of critical flow in large rapids on the Colorado River, Utah. Water Resourc Res 2009:45.
- [6] Preston J. The measurement of pressure in low velocity water flows. J Phys E: Sci Instrum 1972;5:277.
- [7] Boetcher SKS, Sparrow EM. Limitations of the standard Bernoulli equation method for evaluating Pitot/impact tube data. Int J Heat Mass Transf 2007;50:782–8.
- [8] Mckeon B, Li J, Jiang W, Morrison J, Smits A. Pitot probe corrections in fully developed turbulent pipe flow. Meas Sci Technol 2003;14:1449.
- [9] Warzinski RP, Lynn RJ, Robertson AM, Haljasmaa IV. Development of a highpressure water tunnel facility for ocean CO₂ storage experimentation. ACS division of fuel chemistry, preprints of papers. Washington, D.C.: ACS Division of Fuel Chemistry; 2000. p. 809–13.
- [10] Shaffer FD. Method of particle trajectory recognition in particle flows of high particle concentration using a candidate trajectory tree process with variable search areas. US Patent 8,391,552; 2013.
- [11] Shaffer F, Gopalan B, Breault RW, Cocco R, Karri SBR, Hays R, et al. High speed imaging of particle flow fields in CFB risers. Powder Technol 2013;242:86–99.
- [12] Rasband WS. ImageJ. Bethesda, Maryland, USA: US National Institutes of Health; 1997.